Photolabeling Identifies Position 172 of the Human AT_1 Receptor as a Ligand Contact Point: Receptor-Bound Angiotensin II Adopts an Extended Structure†

Antony A. Boucard,‡ Brian C. Wilkes,§ Stéphane A. Laporte,‡ Emanuel Escher,‡ Gaétan Guillemette,‡ and Richard Leduc*,‡

Department of Pharmacology, Faculty of Medicine, Université de Sherbrooke, Sherbrooke, Québec, Canada J1H 5N4, and Clinical Research Institute of Montreal, Montreal, Quebec, Canada H2W 1R7

Received March 15, 2000; Revised Manuscript Received June 6, 2000

ABSTRACT: An angiotensin II (AngII) peptidic analogue in which the third residue (valine) was substituted with the photoreactive *p*-benzoyl-L-phenylalanine (Bpa) was used to identify ligand-binding sites of the human AT_1 receptor. High-affinity binding of the analogue, ^{125}I-[Bpa^3]AngII, to the AT_1 receptor heterologously expressed in COS-7 cells enabled us to efficiently photolabel the receptor. Chemical and enzymatic digestions of the ^{125}I-[Bpa^3]AngII−AT_1 complex were performed, and receptor fragments were analyzed in order to define the region of the receptor with which the ligand interacts. Results show that CNBr hydrolysis of the photolabeled receptor gave a glycosylated fragment which, after PNGase-F digestion, migrated as a 11.4 kDa fragment, circumscribing the labeled domain between residues 143−243 of the AT_1 receptor. Digestion of the receptor−ligand complex with Endo Lys-C or trypsin followed by PNGase-F treatment yielded fragments of 7 and 4 kDa, defining the labeling site of ^{125}I-[Bpa^3]AngII within residues 168−199 of the AT_1 receptor. Photolabeling of three mutant receptors in which selected residues adjacent to residue 168 were replaced by methionine within the 168−199 fragment (I172M, T175M, and I177M) followed by CNBr cleavage revealed that the bound photoligand ^{125}I-[Bpa^3]AngII forms a covalent bond with the side chain of Met^{172} of the second extracellular loop of the AT_1 receptor. These data coupled with previously obtained results enable us to propose a model whereby AngII adopts an extended β-strand conformation when bound to the receptor and would orient itself within the binding domain by having its N-terminal portion interacting with the second extracellular loop and its C-terminus interacting with residues of the seventh transmembrane domain.

The octapeptide hormone angiotensin II (AngII)[1] exerts its diverse effects by interacting with two specific receptor proteins (AT_1 and AT_2) which belong to the heptahelical receptor superfamily (*1*). Both receptors bind AngII with high affinities even though they display a low degree of sequence identity at the amino acid level (34%). The majority of the physiological actions of AngII on cardiovascular, endocrine, and neuronal systems are mediated by the AT_1 receptor that mostly couples to the $G_{q/11}$/phospholipase C/inositol 1,4,5-trisphosphate/cytosolic calcium intracellular signaling pathway (*2*, *3*). Although the functional roles of the AT_2 receptor are not well defined, recent studies have started to delineate a more defined role for this receptor in behavioral and cardiovascular functions as well as in apoptosis (*4*, *5*).

Much effort has gone into investigating the molecular determinants involved in ligand binding to a receptor. The determination of the primary structures of many members of this receptor superfamily has spearheaded the development of multiple strategies to identify regions and residues within receptors that are directly involved in ligand binding. Design and construction of chimeric, mutated, or truncated receptors by mutagenesis coupled with computational approaches have provided evidence as to how interactions between transmembrane domains may be responsible for the formation of a binding pocket and in the bimolecular recognition of receptor and ligand. However, one might argue that such modifications could indirectly affect receptor binding through conformational changes of the receptor (*6*). Thus we sought to use an alternative approach to more directly identify how and precisely where a specific residue of a ligand can interact with various domains/residues within its receptor. Photoaffinity labeling followed by fragmentation of the resulting photoligand−receptor conjugate has been shown to be an important application to directly identify the sites of interaction between a ligand and its cognate receptor. Ligand-binding sites of both bioamine and polypeptide receptors belonging to the heptahelical superfamily have been identified using this technique. For example, the identification of

† This work was supported by grants from the Medical Council of Canada (MRCC) and by the Heart and Stroke Foundation of Canada (HSFC). A.A.J.B. is the recipient of a studentship from FRSQ-FCAR. S.A.L. was the recipient of a HSFC studentship. E.E. is the recipient of the J. C. Edwards Chair in Cardiovascular Research, and R.L. is a scholar from the Fonds de la Recherche en Santé du Québec.

* Corresponding author: tel, 819-564-5413; fax, 819-564-5400; e-mail, rleduc01@courrier.usherb.ca.

‡ Université de Sherbrooke.

§ Clinical Research Institute of Montreal.

[1] Abbreviations: AngII, angiotensin II; Bpa, *p*-benzoyl-L-phenylalanine; BSA, bovine serum albumin; CNBr, cyanogen bromide; Da, dalton; DMEM, Dulbecco's modified Eagle's medium; Endo Lys-C, endoproteinase Lys-C; HPLC, high-performance liquid chromatography; PAGE, polyacrylamide gel electrophoresis; PNGase-F, peptide−*N*-glycosidase F; SP, substance P.

10.1021/bi000597v CCC: $19.00
Published on Web 07/21/2000

ligand−receptor binding domains has been reported for A_1 adenosine (*7*), β_2-adrenergic (*8*, *9*), AT_1 and AT_2 AngII (*10*, *11*), CCK_1 cholecystokinin (*12*, *13*), gonadotropin (*14*), PTH_1 parathyroid hormone (*15*, *16*), secretin (*17*, *18*), NK-1 substance P (*19*), and V_{1a} vasopressin (*20*) receptors. It has been proposed that the binding site of small ligands such as adrenaline to their receptors would be located within the receptor's transmembrane domains (*21*−*23*). In contrast, it is believed that, due to their bulkiness, large protein ligands such as glycoprotein hormones would interact primarily with extracellular domains, more specifically the amino-terminal segment of their cognate receptor (*24*). The binding characteristics of smaller peptides could incorporate some of the features of the bioamines and glycoprotein ligands such that interactions would occur at the level of the extracellular loops and transmembrane domains (*25*). To better define and clarify these principles, precise identification of receptor residues participating in binding becomes essential.

Here, we have substituted the third residue of AngII, normally occupied by valine, with the photoreactive amino acid, *p*-benzoyl-L-phenylalanine. The radioactive analogue ^{125}I-[Bpa^3]AngII was used to covalently label the human AT_1 receptor heterologously expressed in COS-7 cells. Fragmentation of the photolabeled receptor coupled with insertion of methionine residues at key positions enabled us to identify a distinct residue that interacted with the photolabel. This information was crucial to establish a three-dimensional model of how AngII interacts with the AT_1 receptor.

MATERIALS AND METHODS

Materials. Bovine serum albumin, bacitracin, soybean trypsin inhibitor, and cyanogen bromide (CNBr) were from Sigma Chemical Co. (St. Louis, MO). L-158,809 and PD 123319 were generous gifts from Merck and Parke-Davis Warner-Lambert, respectively. Glycopeptidase F (PNGase-F) (EC 3.5.1.52), endoproteinase Glu-C (V8) (EC 3.4.21.19), endoproteinase Lys-C (Endo Lys-C) (EC 3.4.21.50), endoproteinase Arg-C (Endo Arg-C) (EC 3.4.22.8), and trypsin (EC 3.4.21.4) were from Boehringer Mannheim. The cDNA clone of the human AT_1 receptor subcloned in the mammalian expression vector pcDNA3 was kindly provided by Dr. Sylvain Meloche (Université de Montréal). Lipofectamine and culture media were obtained from Life Technologies (Gaithersburg, MD). [Bpa^3]AngII was synthesized in our laboratory by the solid-phase method and purified by high-performance chromatography as previously described (*26*). ^{125}I-AngII and ^{125}I-[Bpa^3]AngII (specific radioactivities ∼1000 Ci/mmol) were prepared with IODOGEN (Pierce Chemical Co.) according to the method of Fraker and Speck (*27*) and as previously reported (*28*).

Site-Directed Mutagenesis. The cDNA encoding the human AT_1 receptor was inserted into *Hin*dIII and *Xba*I sites of M13mp19. Site-directed mutagenesis was done using the Sculptor in vitro mutagenesis kit (Amersham). Three oligonucleotides were constructed to introduce mutations at Ile^{177}, Thr^{175}, and Ile^{172}. The mutagenic primers are the following (altered nucleotides are underlined): Ile^{177}→Met (hAT_1I177M), 5-GCACAAACTGTCATATTGGTGTTC-3; Thr^{175}→Met (hAT_1T175M), 5-CAAACTGTAATATTCATGTTCTCAATG-3; Ile^{172}→Met (hAT_1I172M), 5-GGTGTTCTCCATGAAAAATACA-3. After confirmation of site-directed mutation by DNA sequencing, the hAT_1I177M, hAT_1T175M, and hAT_1I172M cDNAs were excised from the M13mp19RF form by digestion with *Hin*dIII and *Xba*I and subcloned into the multiple cloning site of pcDNA3 that had been digested by these same restriction enzymes.

Cell Culture and Transfections. COS-7 cells were grown in Dulbecco's modified Eagle's medium (DMEM) containing 2 mM L-glutamine and 10% (v/v) fetal bovine serum. Cells were seeded into 75 cm^2 culture dishes at a density of 25 000 cells/cm^2. When cells reached ∼70% confluency, they were washed once with PBS and infected for 1 h using a recombinant vaccinia virus (4.07×10^7 pfu/μL) expressing T7 DNA polymerase with a multiplicity of infection of 2. The cells were then washed with serum-free DMEM and transfected with 4 μg of plasmid DNA and 25 μL of lipofectamine in 8 mL of serum-free DMEM. The cells were incubated for 5 h at 37 °C, and the media were replaced with a complete DMEM medium containing 100 IU/mL penicillin and 100 μg/mL streptomycin. Transfected cells were grown for 24 h before photoaffinity labeling and binding assays.

Binding Experiments. Cell membrane preparation and binding assays were performed essentially as previously described (*29*). Briefly, COS-7 cells were grown for 24 h postinfection in 100 mm plates, washed once with PBS, and subjected to one freeze−thaw cycle. Broken cells were then gently scraped in washing buffer (25 mM Tris-HCl, pH 7.4, 5 mM $MgCl_2$, 100 mM NaCl), centrifuged at 2500*g* for 10 min at 4 °C, and resuspended in binding buffer (25 mM Tris-HCl, pH 7.4, 5 mM $MgCl_2$, 100 mM NaCl, 1% BSA, 0.01% bacitracin). Broken cells (25−70 μg of protein) were incubated for 1 h at room temperature in binding buffer containing increasing concentrations of ^{125}I-[Sar^1,Ile^8]AngII or ^{125}I-[Bpa^3]AngII in a final volume of 0.5 mL. Bound radioactivity was separated from free ligand by filtration through GF/C filters presoaked for 1 h in binding buffer. Nonspecific binding was measured in the presence of 1 μM unlabeled AngII. Receptor-bound radioactivity was evaluated by γ counting.

Photoaffinity Labeling. Transfected COS-7 cells were photolabeled as previously described (*30*). Briefly, cells were incubated in 1 mL of binding buffer containing 0.01% soybean trypsin inhibitor and the photoreactive radioligand (5 nM), in the presence or absence of L-158,809 (1 μM) (an AT_1 selective nonpeptide analogue) or PD 123319 (10 μM) (an AT_2 selective nonpeptide analogue). After 1 h at room temperature, cells were washed with 20 mL of ice-cold washing buffer and irradiated for 60 min at 0 °C under filtered UV light (365 nm) (mercury vapor lamp, serial number JC-Par-38 from Westinghouse, and Raymaster black light filters, number 5873 from Gates and Co. Inc., Long Island, NY). Cells were then gently scraped and centrifuged (200*g*) for 10 min at 4 °C. The pellet was solubilized in a buffer containing 100 mM Na_2HPO_4, pH 8.5, 25 mM EDTA, 0.1 mg/mL soybean trypsin inhibitor, and 1% (v/v) Nonidet P-40. After centrifugation (13000*g* for 10 min at 4 °C), the supernatants were kept at −20 °C until further analysis.

Partial Purification of the Labeled Complex. The solubilized photolabeled receptors were diluted with an equal volume of 2 × loading buffer [120 mM Tris-HCl, pH 6.8, 20% (v/v) glycerol, 4% (w/v) SDS, 200 mM dithiothreitol, and 0.05% (w/v) bromophenol blue] and incubated for 1 h

at 37 °C. SDS−polyacrylamide gel electrophoresis (PAGE) was performed as described by Laemmli (*46*) using 1.5 mm 8% gels. The gel was then dried and exposed to X-ray film (Kodak XAR-5) with an intensifying screen. The labeled proteins were isolated from the preparative gel using a passive elution protocol similar to that described by Blanton and Cohen (*31*). After autoradiography, radioactive bands were excised from dried gels and rehydrated with appropriate digestion buffer. The gel slices were macerated and eluted with 5 mL of buffer for 3−4 days at 4 °C under gentle agitation. Under these conditions we repeatedly recovered at least 80% of the initial radioactivity. The eluted proteins were filtered (0.22 μm), and the gel slices were washed with 10 mL of digestion buffer. The whole gel eluate (12−15 mL) was concentrated approximately 150 times using Centriprep-10 and Centricon-10 (Amicon), and the partially purified proteins were aliquoted in fractions of (1−2) × 10^5 cpm and kept at −20 °C.

Endoglycosidase, Proteolytic, and Chemical Digestions. For endoglycosidase digestions, partially purified photolabeled receptors were resuspended in digestion buffer containing 0.5% (v/v) Nonidet P-40. PNGase-F (33−100 units/mL) was added, and samples were incubated at room temperature for 16 or 3 h at 37 °C. For proteolytic digestions, partially purified photolabeled receptors (5000−20 000 cpm) were resuspended in 25 μL of digestion buffer containing 100 mM NH_4HCO_3, pH 8.0, and 0.1% (w/v) SDS. Under these conditions V8 protease is known to cleave at the carboxy-terminal end of glutamate residues. Samples were incubated for 5−7 days at room temperature with the indicated amounts of V8 protease. Partially purified photolabeled receptors (5000−20 000 cpm) were also digested for 16−24 h at 37 °C with the indicated amount of Endo Lys-C in 25 μL of digestion buffer containing 25 mM Tris-HCl, pH 8.5, 1 mM EDTA, and 0.1% SDS. For Endo Arg-C digestions, photolabeled receptors (5000−20 000 cpm) were resuspended in 25−55 μL of digestion buffer containing 90 mM Tris-HCl, pH 7.6, 8.5 mM $CaCl_2$, 5 mM DTT, 0.5 mM EDTA, and 0.01% SDS. Indicated amounts of Endo Arg-C were added, and samples were incubated for 16 h at 37 °C. Trypsin digestions were performed at 37 °C for 16 h with the indicated amount after resuspension of the photolabeled receptors (5000−10 000 cpm) in digestion buffer containing 100 mM Tris-HCl, pH 8.5, 10 mM $CaCl_2$, and 0.1% SDS. All digestions were terminated by addition of an equal volume of 2 × loading buffer (previously described) and boiling the samples for 3 min. When subsequent digestions were needed, products of the first digestion were concentrated using Microcon-3 (Amicon) and diluted with the appropriate digestion buffer. Concentrated proteins were submitted to chemical and enzymatic cleavage as described. For CNBr hydrolysis, partially purified photolabeled receptors (5000−10 000 cpm) were resuspended in 200 μL of 70% (v/v) trifluoroacetic acid, and CNBr (200 μL) was added to a final concentration of 100 mg/mL. Samples were incubated at room temperature, in the dark, for 18 h. Reactions were terminated by addition of 1−4 mL of water. Samples were lyophilized, resuspended in denaturing buffer, and analyzed by SDS−PAGE.

Analysis of Products of Proteolysis and Chemical Cleavage. The products of proteolysis and chemical cleavage were analyzed by SDS−PAGE using 16.5% Tris−Tricine gels (Bio-Rad) followed by autoradiography on X-ray films (Kodak BioMax MS) with intensifying screens. ^{14}C-Labeled low molecular mass protein standards (Amersham Inc.) were used to determine apparent molecular masses. Running conditions, fixation, and coloration of gels were performed according to the manufacturer's instructions.

Molecular Modeling. All calculations were performed using the software package SYBYL (Tripos Associates, St. Louis, MO) on a Silicon Graphics Indigo^2 extreme workstation. The Tripos force field was used for energy calculations (*32*) with a dielectric constant of 1. Charges were calculated according to the method of Gasteiger (*33*). The model for the seven transmembrane domain protein was constructed on the basis of the sequence alignment of Yamano et al. (*34*), using the helix arrangement based on the rhodopsin family of transmembrane proteins proposed by Schwartz et al. (*35*). The extracellular loops were attached to the α-helices as flexible chains with no constraints on their conformation other than the requirement for a disulfide bond between cysteine residues in the first two extracellular loops (*35*). The side chains of each individual amino acid were packed using the scan subroutine in SYBYL. In this procedure, the backbone dihedral angles were held fixed, while the side chain dihedral angles were rotated one at a time until a sterically acceptable conformation was obtained. At this point AngII was inserted into the receptor in an extended conformation. No constraints were used to enforce the extended conformation of the ligand, but three distance constraints were imposed to ensure close proximity between Val^3 of the ligand and Ile^{172} of the receptor and between Phe^8 of the ligand and Phe^{293} and Asn^{294} of the receptor. At this point the entire ligand−receptor complex was minimized, allowing all atoms to relax. This complex was then subjected to 20 ps of molecular dynamics simulation. Changes in secondary structural elements and distances between selected amino acids were monitored. There were no major changes in the secondary structures during the simulation.

RESULTS

Binding Specificity of the Photoreactive Analogue. Figure 1 shows the primary structure of AngII, the photoreactive AngII analogue, and the sequence of the human AT_1 receptor used in this study. Val at position 3 of AngII was replaced by Bpa to give [Bpa^3]AngII. In saturation binding assays, [Bpa^3]AngII exhibited high affinities for the AT_1 receptor expressed in COS-7 cells with a K_d value of 0.52 ± 0.09 nM. This is similar to the affinity of AngII for AT_1 (1.13 ± 0.12 nM) in these conditions. The functional properties of this particular analogue were then analyzed by the measurement of the ligand-induced inositol 1,4,5-trisphosphate production in COS-7 cells expressing the AT_1 receptor. Incubation of the cells with a high concentration of [Bpa^3]-AngII or AngII (1 μM) activated phospholipase C and caused an increase of inositol 1,4,5-trisphosphate production (20 135 ± 1273 and 35 735 ± 1170 cpm over basal, respectively), thus demonstrating the agonistic nature of the analogue. In photoaffinity labeling experiments, ^{125}I-[Bpa^3]AngII specifically labeled the hAT_1 receptor that migrated as a glycoprotein of 110 kDa (Figure 2, lane 1), as previously described (*28*). The labeling of the hAT_1 receptor by the analogue was completely abolished by L-158,809 (1 μM) (Figure 2, lane 2), a selective AT_1 receptor ligand, and by AngII (1 μM)

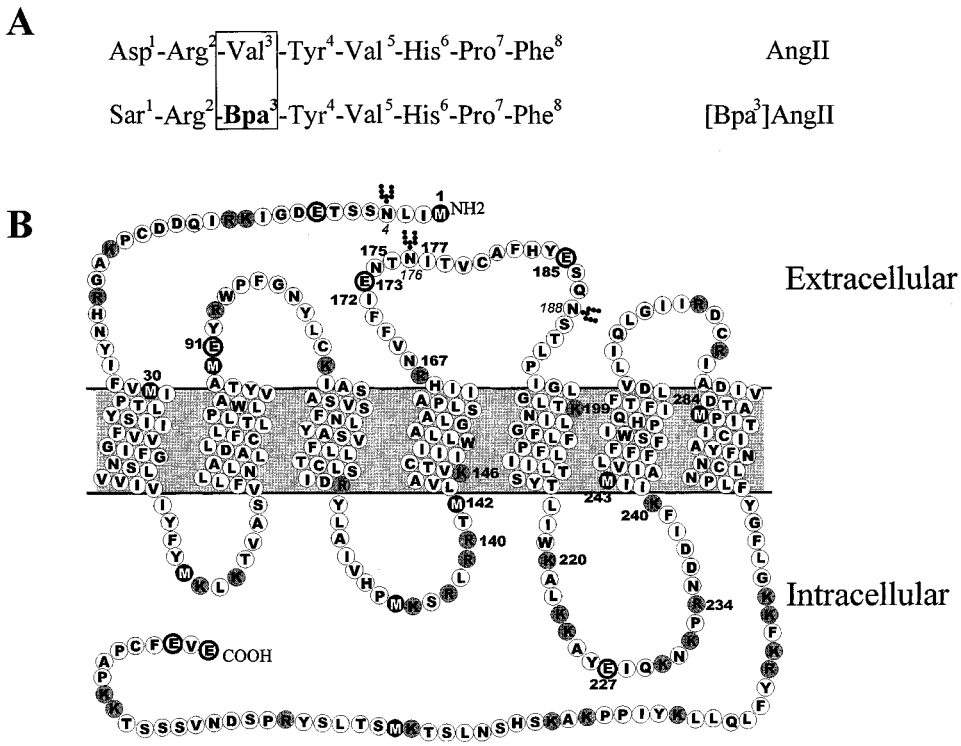

FIGURE 1: (A) Amino acid sequence of the photoreactive AngII analogue. Residues represented in bold characters correspond to amino acid modifications. (B) Two-dimensional representation of the primary structure of the human AT_1 receptor and its potential sites of cleavage by specific proteases and CNBr. Black closed circles indicate sites of hydrolysis for CNBr. Bold circles indicate recognition sites for V8 protease. K indicates recognition sites for Endo Lys-C. R indicates recognition sites for Endo Arg-C. Gray closed circles indicate recognition sites for trypsin. Putative sites of N-glycosylation on asparagines 4, 176, and 188 are also indicated.

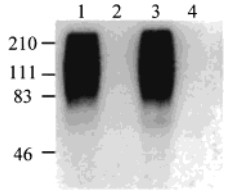

FIGURE 2: Photoaffinity labeling of the human AT_1 receptor expressed in transfected COS-7 cells. After photolabeling, cellular proteins were solubilized, denatured, and submitted to SDS−PAGE on a 8% acrylamide separating gel (40 μg of protein per lane) followed by autoradiography. Lanes 1−4, ^{125}I-[Bpa^3]AngII-labeled proteins. Lane 1, total labeling; lane 2, labeling in the presence of AngII (1 μM); lane 3, labeling in the presence of PD 123319 (10 μM); lane 4, labeling in the presence of L-158,809. Protein standards of the indicated molecular masses (in kDa) were run in parallel. These results are representative of at least three separate experiments.

(Figure 2, lane 4) but not with PD-123319 (10 μM) (Figure 2, lane 3), an AT_2 selective ligand, thereby confirming the specificity and the selectivity of the labeling. Determination of covalent incorporation yields, calculated from the ratio of total radioactivity found in isolated bands to total specific binding observed before photolysis, revealed that ^{125}I-[Bpa^3]-AngII had a 60% yield of covalent incorporation onto the hAT_1 receptor.

Mapping the ^{125}I-[Bpa^3]AngII Contact Points on AT_1. To identify the binding domain, the photolabeled receptor (Figure 3A, lane 1) was partially purified as indicated in the Materials and Methods section and submitted to cyanogen bromide (CNBr), which cleaves on the C-terminal side of methionine residues. This chemical digestion produced a broad band of 45 kDa, suggesting the presence of a glycosylated fragment (Figure 3A, lane 2). Treatment of the

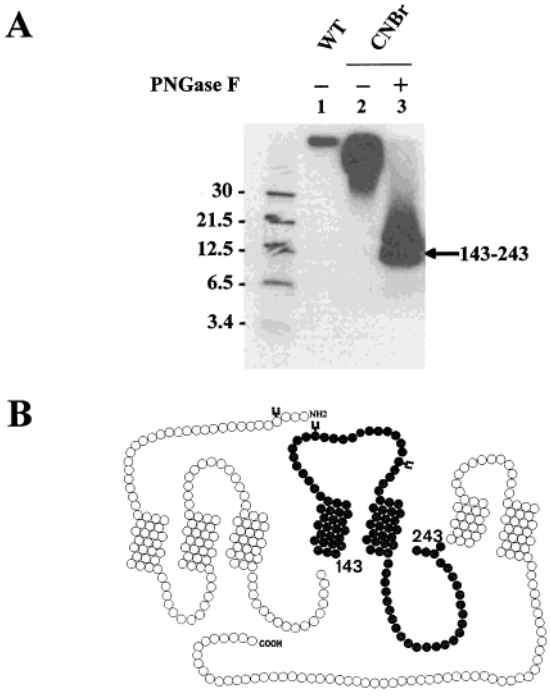

FIGURE 3: CNBr hydrolysis of ^{125}I-[Bpa^3]AngII-labeled AT_1 receptor. (A) Partially purified photolabeled AT_1 receptor (10 000 cpm) was incubated in the absence (lane 1) or presence (lanes 2 and 3) of CNBr (100 mg/mL) for 18 h at room temperature in the dark and deglycosylated using PNGase-F (2 units) digestion (lane 3). Samples were run on a 16.5% acrylamide−Tris−Tricine separating gel followed by autoradiography. ^{14}C-Labeled protein standards of the indicated molecular masses (in kDa) were run in parallel. These results are representative of three separate experiments. (B) The two-dimensional representation of the hAT_1 receptor shows the CNBr-generated fragment in gray closed circles.

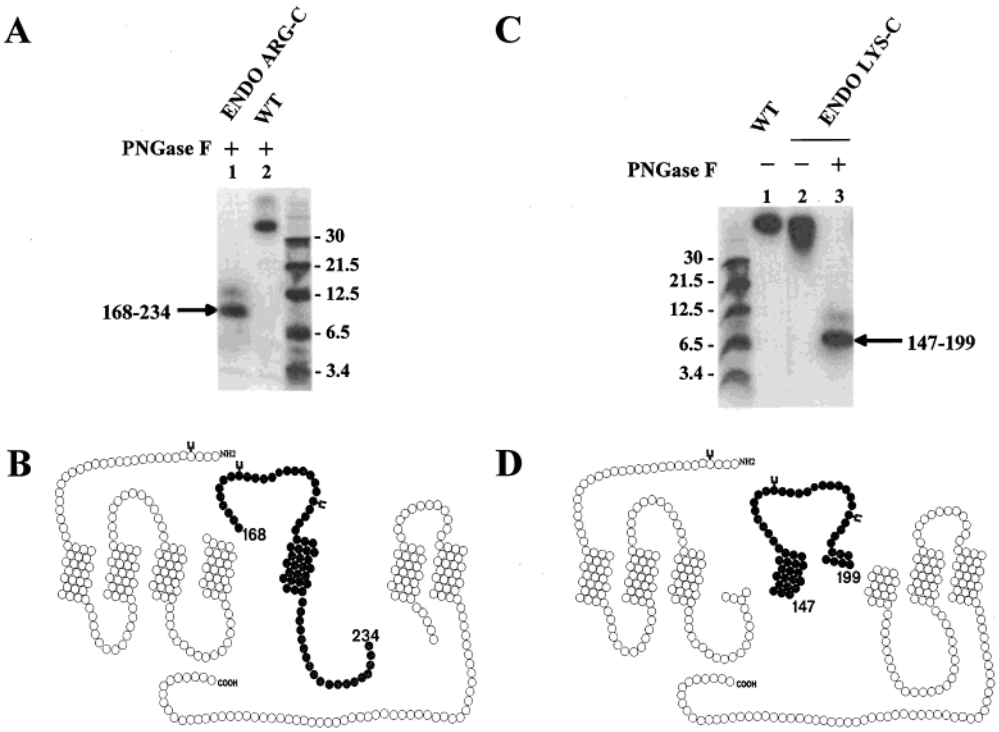

FIGURE 4: Endo Arg-C and Endo Lys-C digestion of ^{125}I-[Bpa^3]AngII-labeled AT_1 receptor. (A) Partially purified photolabeled AT_1 receptor (5 000 cpm) was incubated with PNGase-F (2 units) for 3 h at 37 °C. The deglycosylated complex was then incubated in the presence (lane 1) or the absence (lane 2) of Endo Arg-C (0.5 μg) for 16 h at 37 °C. The two-dimensional representation of the hAT_1 receptor shows the Endo Arg-C generated fragment in gray closed circles. (B) Partially purified photolabeled AT_1 receptor (5 000 cpm) was incubated in the absence (lane 1) or presence (lanes 2 and 3) of Endo Lys-C (5 μg) at 37 °C for 16 h. Resulting fragments were treated without (lane 2) or with (lane 3) PNGase-F for 16 h at room temperature. The two-dimensional representation of the hAT_1 receptor shows the Endo Lys-C generated fragment in gray closed circles. All samples were run on a 16.5% acrylamide−Tris−Tricine separating gel followed by autoradiography. ^{14}C-Labeled protein standards of the indicated molecular masses (in kDa) were run in parallel. These results are representative of three separate experiments.

45 kDa CNBr fragment with PNGase-F confirmed the glycosylated nature of the polypeptide and yielded a 12.5 kDa fragment (Figure 3A, lane 3). The only candidate fragment corresponding to this size is one of 101 residues encompassing Leu^{143} and Met^{243} (Figure 3B).

To confirm the identity of the domain interacting with ^{125}I-[Bpa^3]AngII, the ^{125}I-[Bpa^3]AngII−AT_1 complex was first digested with PNGase-F. This treatment shifted the mobility of the ^{125}I-[Bpa^3]AngII−hAT_1 receptor complex to an apparent molecular mass (M_r) of 34 kDa, corroborating the glycosylated nature of hAT_1 receptor (Figure 4A, lane 2). Digestion of the deglycosylated photolabeled receptor with endoproteinase Arg-C, which specifically cleaves peptide bonds on the C-terminal side of arginine residues, produced a fragment of 8.9 kDa (Figure 4A, lane 1). On the basis of this apparent molecular mass and upon inspection of the primary structure of the receptor, we delineated two possible photolabeled peptides corresponding to His^{24}−Arg^{93} or Asn^{168}−Arg^{234}. However, digestion of the glycosylated ligand−receptor complex first by Arg-C and then by a PNGase step, which revealed a shift in the mobility of the fragment, clearly indicated to us the glycosylated nature of the fragment produced (data not shown). This strongly points toward a labeling of the Asn^{168}−Arg^{234} fragment since the glycosylation sites are located at Asn^4, Asn^{176}, and Asn^{188} (*36*). These results combined with the CNBr cleavage of the complex indicated that the ligand-binding regions must reside within the second extracellular loop and the fifth transmembrane domain.

To map the labeled region more precisely, we submitted the ^{125}I-[Bpa^3]AngII−AT_1 complex to Endo Lys-C digestion, which specifically cleaves on the carboxylic side of lysine residues. Taking into account that the labeled fragment must overlap with Asn^{168}−Arg^{234}, the two possible peptides would be the glycosylated Val^{147}−Lys^{199} or the nonglycosylated Asn^{200}−Lys^{220}. Following Endo Lys-C digestion, we were able to identify a glycosylated fragment (Figure 4C, lane 2) which migrated as a 7 kDa fragment when treated with PNGase-F (Figure 4C, lane 3). From this experiment, we can clearly establish the labeling site to be located between Val^{147} and Lys^{199}. Together with the results obtained with the Endo Arg-C digestion, the smallest deduced peptide with which the photoligand can interact would be Asn^{168}−Lys^{199}. Essentially, this fragment constitutes the second extracellular loop of the AT_1 receptor.

To further confirm the labeling site, we used trypsin digestions on the complex to cleave at both Arg^{167} and Lys^{199}. Once again we verified the glycosylated nature of the produced fragment. Trypsin proteolysis of the ^{125}I-[Bpa^3]-AngII−AT_1 conjugate led to the production of a glycosylated fragment (Figure 5A, lane 2) which, after deglycosylation, revealed the presence of a 7 kDa and a 4.1 kDa fragment (Figure 5A, lane 3). This pattern could correspond to an incomplete digestion of the complex, yielding both the Val^{147}−Lys^{199} and Asn^{168}−Lys^{199} fragments, respectively. This was indeed the case since the 7 kDa fragment disappeared after extended digestion periods and only the 4.1 kDa remained (data not shown).

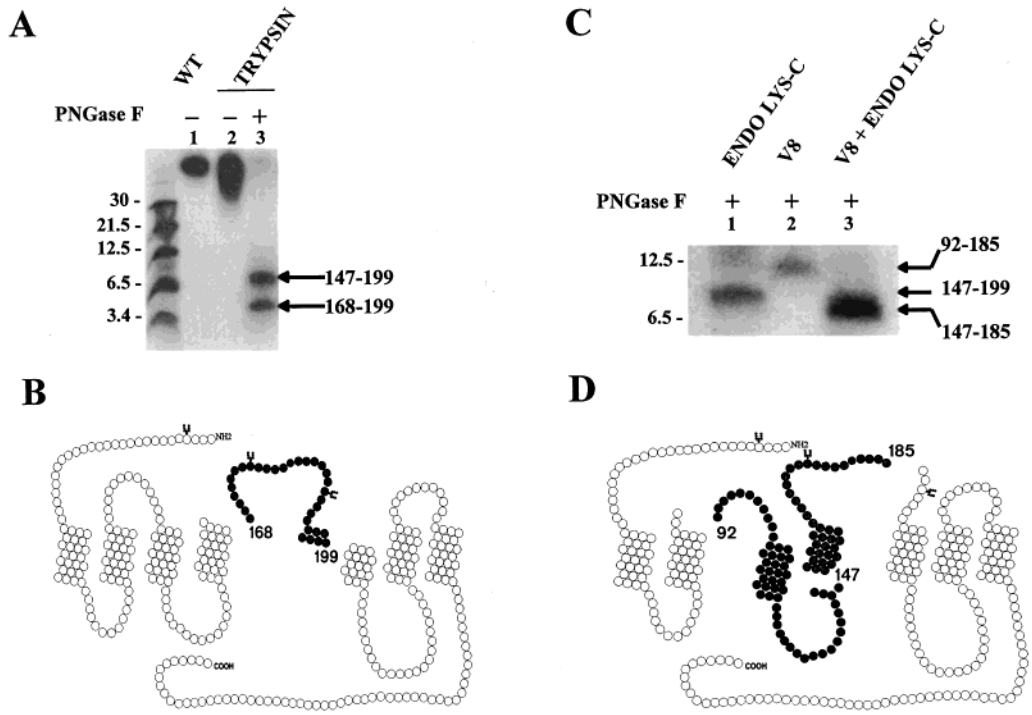

FIGURE 5: Trypsin and V8 protease digestion of ^{125}I-[Bpa^3]AngII-labeled AT_1 receptor. (A) Partially purified photolabeled AT_1 receptor (5 000 cpm) was incubated in the absence (lane 1) or the presence (lanes 2 and 3) of trypsin (10 μg) at 37 °C for 16 h. Resulting fragments were treated without (lane 2) or with (lane 3) PNGase-F for 16 h at room temperature. The two-dimensional representation of the hAT_1 receptor shows the trypsin-generated fragment in gray closed circles. (B) Partially purified photolabeled AT_1 receptor (5 000 cpm) was incubated with PNGase-F (2 units) for 3 h at 37 °C (lanes 1−3). Endo Lys-C (5 μg) (lane 1) or V8 protease (20 μg) (lane 2) was added, and the incubation was prolonged for 24 h at 37 °C and 7 days at room temperature, respectively. The 11.6 kDa labeled receptor fragment (lane 2) was recovered after dialysis of the V8 protease digestion using Microcon-3 (cutoff of 3 kDa). The labeled receptor fragment was split in two aliquots and was incubated in the absence (lane 2) or presence of Endo Lys-C (lane 3) for 16 h at 37 °C. The two-dimensional representation of the hAT_1 receptor shows the V8 protease fragment in black circles. The fragment generated by Endo Lys-C digestion of the V8 protease fragment is represented in gray closed circles. The samples were run on a 16.5% acrylamide−Tris−Tricine separating gel followed by autoradiography. ^{14}C-Labeled protein standards of the indicated molecular masses (in kDa) were run in parallel. These results are representative of three separate experiments.

We took advantage of the presence of two glutamic acid residues, Glu^{173} and Glu^{185} (Figure 2), in the identified domain, which represent suitable sites for cleavage with V8 protease, to better define the binding site. We had found that the extent of V8 protease digestion was greater when the glycosylation sites (Asn^{176} and Asn^{188}) were unoccupied (data not shown), this possibly due to steric hindrance of the sugar moieties. Thus, we submitted the deglycosylated ^{125}I-[Bpa^3]-AngII−AT_1 complex to V8 protease digestion, which led to the production of an 11.6 kDa fragment (Figure 5C, lane 2) corresponding to the Tyr^{92}−Glu^{185} polypeptide. Confirmation of this fragment was done by incubating the 11.6 kDa fragment with Endo Lys-C, which led to the production of a 6 kDa band identified as Val^{147}−Glu^{185} (Figure 5C, lane 3). Notice how the 6 kDa fragment compares to the 53 residue, 7 kDa Val^{147}−Lys^{199} peptide produced by Endo Lys-C digestion (Figure 5C, lane 1). Together, these results show that ^{125}I-[Bpa^3]AngII potentially labels a residue found within Asn^{168}−Glu^{185} of the AT_1 receptor.

Ile^{172} Interacts with ^{125}I-[Bpa^3]AngII. To precisely identify the interacting domain/residue of ^{125}I-[Bpa^3]AngII to AT_1, we constructed a series of mutant receptors where methionine residues individually replaced amino acids found at positions 172, 175, and 177. We initially examined the binding characteristics of the AT_1I177M mutant, which were essentially similar to those of the wild-type receptor with a K_d of 1.15 ± 0.11 nM (data not shown). Production of inositol 1,4,5-trisphosphate following addition of 1 μM AngII or [Bpa^3]AngII revealed the functionality of this receptor (data not shown). The mutant receptor was photolabeled with ^{125}I-[Bpa^3]AngII, and the resulting complex was deglycosylated (Figure 6A, lane 1). Use of CNBr led to the generation of a 5 kDa fragment (Figure 6A, lane 2) corresponding to Leu^{143}−Met^{177}. These results further delineate the labeled peptide to residues 168−177 of the AT_1 receptor, which is the N-terminal region of the second extracellular loop of the receptor.

The two other Met mutants (AT_1I172M and AT_1T175M) also demonstrated good affinities for [Sar^1,Ile^8]AngII (2 and 1 nM, respectively) while AngII and [Bpa^3]AngII retained their agonistic properties on these two receptors. We first confirmed the glycosylated nature of the AT_1T175M by submitting the photolabeled complex to PNGase-F digestion (Figure 6B, lane 2). CNBr cleavage of ^{125}I[Bpa^3]AngII−AT_1-T175M yielded a nonglycosylated 5 kDa band (Figure 6B, lane 3) corresponding to a fragment between Leu^{143} and Met^{175} and further circumscribing the interaction domain between Asn^{168}−Thr^{175}. Interestingly, CNBr cleavage alone of the ^{125}I[Bpa^3]AngII−AT_1I172M complex led to the production of an aglycosylated 2 kDa band (Figure 6C, lane 2) which comigrated with the native photoligand (^{125}I[Bpa^3]-AngII, ∼1 kDa) that was run in parallel (Figure 6C, lane 5). Cleavage by both CNBr and PNGase-F of the photoligand−mutant receptor conjugate yielded a band of 12.5 kDa (Figure

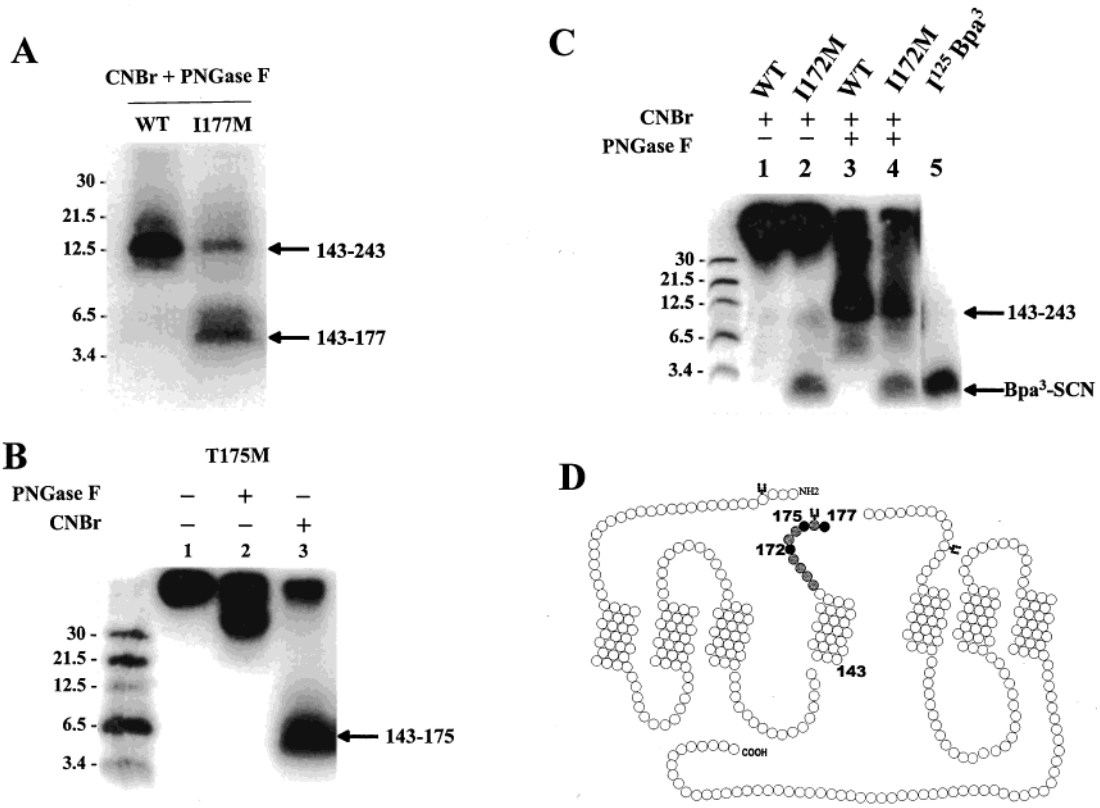

FIGURE 6: CNBr cleavage of hAT_1 mutant receptors. (A) Partially purified photolabeled hAT_1 (lane 1) and hAT_1I177M (lane 2) receptors (2 000 cpm) were incubated in the presence of CNBr (100 mg/mL) for 18 h at room temperature in the dark and deglycosylated using PNGase-F (2 units) digestion. (B) Partially purified photolabeled hAT_1T175M (lane 1) receptor (3 000 cpm) was deglycosylated using PNGase-F (2 units) digestion (lane 2) or incubated in the presence of CNBr (100 mg/mL) for 16 h at room temperature in the dark (lane 3). (C) Partially purified photolabeled hAT_1 (lanes 1 and 3) and hAT_1I172M (lanes 2and 4) receptors (3 000 cpm) were incubated in the presence of CNBr (100 mg/mL) for 18 h at room temperature in the dark. Resulting fragments were then incubated in the absence (lanes 1 and 2) or presence (lanes 3 and 4) of PNGase-F (2 units). In lane 5, the ^{125}I-[Bpa^3]AngII supplemented with 10 μg of BSA was run in parallel. The samples were run on a 16.5% acrylamide−Tris−Tricine separating gel followed by autoradiography. ^{14}C-Labeled protein standards of the indicated molecular masses (in kDa) were run in parallel. These results are representative of three separate experiments. (D) Schematic representation of the CNBr resulting fragments on the methionine mutant receptors and the domain circumscribed by the mutant receptors.

6C, lane 4). Understanding that a labeling occurring N-terminal to I^{172} would give a 5 kDa nonglycosylated fragment (residues 143−172) and that labeling C-terminal to I^{172} would give a glycosylated 9.3 kDa fragment (residues 173−243), the only possibility for the 2 kDa fragment is the presence of the cleaved, thiocyanate photoligand (see Discussion). The presence of the 12.5 kDa fragment can be explained by a partial CNBr cleavage of M^{172} in the I172M receptor, which will generate the L^{143}−M^{243} fragment.

DISCUSSION

Elucidation of the mechanisms by which a ligand recognizes its receptor is an important goal in understanding the mode of action of bioactive compounds. Moreover, identifying the molecular determinants involved in this process will aid in delineating the principles of bimolecular recognition/interaction and receptor activation. In the present study, using photoaffinity labeling and site-directed mutagenesis, we examined and identified the amino acid of the AT_1 receptor which interacts with the photoreactive analogue [Bpa^3]AngII. The high affinity of the [Bpa^3]AngII analogue (0.6 nM) for AT_1 contributed to the high-yield incorporation (60%) of the radioactive photoligand and facilitated our mapping studies. Production of the second messenger inositol 1,4,5-trisphosphate by [Bpa^3]AngII led to the conclusion that the analogue was an agonist, which is in agreement with structure−activity studies that showed how position 3 (occupied by Val in AngII) can be rather permissive and can accommodate a variety of natural and nonnatural residues often leading to production of agonists (*37*).

Working with the photolabeled wild-type receptor and using consecutive and reciprocal treatment with Endo Arg-C and PNGase-F along with a combination of V8 protease followed by Lys-C digestions, we were able to show that the shortest generated fragment to which [Bpa^3]AngII can bind was the Asn^{168}−Glu^{185} polypeptide. Essentially, this corresponds to the N-terminus of the second extracellular loop of AT_1. Mutagenesis studies performed on this region of the AT_1 receptor had previously shown how segment substitutions or specific residue changes such as Val^{179}→Ala, Arg^{167}→Ala, or Cys^{180}→Gly that abolishes a disulfide bridge could impair peptide binding (*38*, *39*). Moreover, it was suggested that His^{183} of AT_1 interacts with the carboxylate of Asp at position 1 of AngII (*40*). Therefore, our results showing that [Bpa^3]AngII can interact with elements of the second extracellular loop of AT_1 are consistent with these reported observations.

In an attempt to identify the residue to which the analogue interacted, we used a method adapted from an observation made by Kage et al., where a methionine-bound photoligand

can be released from its receptor following CNBr cleavage (*41*). Indeed, interaction of the ketone group of the benzophenone moiety of the photoreactive analogue with the ϵ-methyl group of a Met residue will form an adduct that, when exposed to CNBr, will release the ligand as a thiocyanate-modified product. This compound should be observed on SDS−PAGE with a molecular mass (~1 kDa) indistinguishable from that of ^{125}I[Bpa^3]AngII. This pattern of ligand release when interacting with methionine has been observed in the case of the substance P (NK-1) receptor (*41*) and the parathyroid hormone receptor subtypes (PTH-1 and PTH-2) (*42*, *43*). Therefore, we took advantage of the fact that the Asn^{168}−Glu^{185} region does not possess Met residues to introduce methionine at specific positions within this fragment in order to pinpoint the position of the photolabel. Analysis of the wild-type and the three mutant receptors incorporating Met revealed that only hAT_1I172M released the ligand upon CNBr cleavage. This suggests that, upon binding, the third position of the analogue [Bpa^3]AngII interacts with the ϵ-methyl of Met^{172}. By extension, the wild-type Ile residue of position 172 could possibly be located at the junction of the fourth transmembrane domain and the second extracellular loop of the hAT_1 receptor and serve as a hydrophobic interaction site with the Val of the third position of AngII. Whether the interaction observed with the photoreactive analogue is identical to the one achieved by the natural AngII remains arguable but highly plausible since results such as similar pharmacological properties of [Bpa^3]-AngII vs AngII and extensive SAR studies on AngII would favor similar positioning of both ligands within the binding pocket.

We had recently shown how two other photosensitive analogues, [Bpa^1]AngII and [Bpa^8]AngII, interacted with a fragment encompassing the second extracellular loop of the receptor and an 11-residue fragment (Pro^{285}−Asn^{295}) in the middle of the seventh transmembrane domain, respectively (*11*). Site-directed mutagenesis studies suggested that Asn^{294} was an essential determinant of receptor activation while the adjacent Asn^{295} is required for normal ligand binding (*44*). These results support recent experiments by our group, whereby the [Bpa^8]AngII analogue would directly interact with Phe^{293} or Asn^{294} of the AT_1 receptor (manuscript in preparation). Thus, we have identified two anchor points by our photoaffinity approach using the [Bpa^3]AngII and [Bpa^8]-AngII analogues and have gained information that [Bpa^1]-AngII would interact with the second extracellular loop of the receptor. Using these data, we constructed a model of AngII bound to the AT_1 receptor. Homology modeling was based on the rhodopsin family of seven transmembrane proteins (*33*). In this model the distance between Ile^{172} of the second extracellular loop and Phe^{293}/Asn^{294} of the seventh transmembrane domain was found to be approximately 26 Å. To accommodate this distance, AngII was constructed in an extended β-strand conformation. AngII was inserted into the receptor, allowing for close contact between Val^3 of AngII and Ile^{172} of the receptor as well as close contact between Phe^8 of AngII and Phe^{293}/Asn^{294} of the receptor. Minimization and a molecular dynamics simulation demonstrated that no major conformational changes occurred in the secondary structures of the ligand or receptor, suggesting that this complex is stable and contains no unfavorable steric interactions. Moreover, AngII maintains a β-strand conformation and positions itself in the binding pocket of the receptor surrounded by transmembrane helices 2, 3, 5, 6, and 7 (Figure 7).

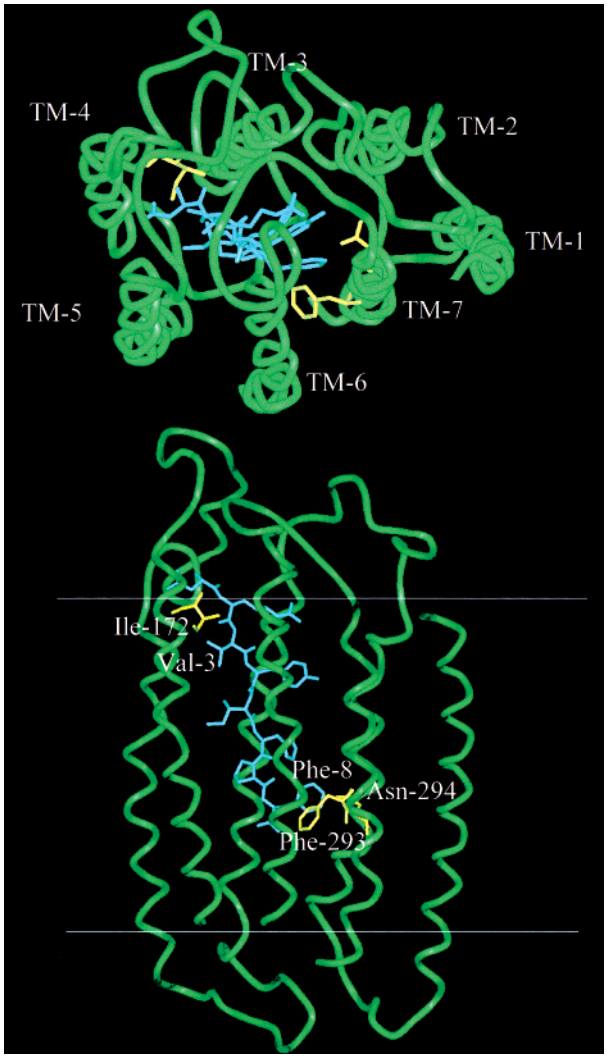

FIGURE 7: Molecular modeling of the AT_1 receptor binding pocket and its AngII contact sites. The receptor backbone is displayed in green. AngII and key receptor residues are highlighted in light blue and yellow, respectively. Amino acid residues Val^3 and Phe^8 of AngII are indicated adjacent to the side chains while Ile^{172}, Phe^{293}, and Asn^{294} of AT_1 are also shown. The top panel is viewed from the top of the membrane, and the bottom panel is viewed in the plane of the membrane.

Similar patterns of interactions have been described with other peptidic or polypeptidic ligand−receptor complexes. Using a photoaffinity labeling technique, Li et al. have shown that the carboxyl-terminal hydrophobic sequence of substance P (SP) inserts into a hydrophobic ligand-binding pocket localized into the upper part of the murine neurokinin NK-1 receptor transmembrane domains while the remainder of the SP molecule interacts with ectodomains of the receptor including the second extracellular loop (*45*). The authors proposed a model in which the carboxyl-terminal end of the peptide positions itself between helices in the outer part of plasma membrane whereas the amino-terminal portion of the peptide is stabilized by ectodomains of the NK-1 receptor.

In conclusion, this study has identified Ile^{172} of the AT_1 receptor as the residue with which Val^3 of AngII can putatively interact. On the basis of these and other results, we propose a model where AngII adopts an extended

structure where the amino terminus of the hormone interacts with elements of the second extracellular loop and the carboxyl terminus interacts with residues of the seventh TM. The hormone AngII would thus penetrate a binding pocket created mostly by TMs 3, 5, 6, and 7. This interaction pattern, also found in other G-protein-coupled receptors for small bioactive peptides, may correspond to a highly conserved feature among this very large family of receptors. By using different photosensitive analogues of AngII, it will be possible to bring additional information in order to refine the molecular model of the AT_1 receptor binding pocket.

REFERENCES

1. Timmermans, P. B., Wong, P. C., Chiu, A. T., Herblin, W. F., Benfield, P., Carini, D. J., Lee, R. J., Wexler, R. R., Saye, J. A., and Smith, R. D. (1993) *Pharmacol. Rev. 45*, 205−251.
2. Matsusaka, T., and Ichikawa, I. (1997) *Annu. Rev. Physiol. 59*, 395−412.
3. Catt, K. J., Sandberg, K., and Balla, T. (1993) in *Cellular and Molecular Biology of the Renin−Angiotensin System* (Raizada, M., Phillips, M. I., and Sumners, C., Eds.) pp 307−356, CRC Press, Boca Raton, FL.
4. Nahmias, C., and Strosberg, A. D. (1995) *Trends Pharmacol. Sci. 16*, 223−225.
5. Matsubara, H. (1998) *Circ. Res. 83*, 1182−1191.
6. Schwartz, T. W., Perlman, S., Rosenkilde, M. M., and Hjorth, S. A., (1997) *Ann. N.Y. Acad. Sci. 812*, 71−84.
7. Kennedy, A. P., Mangum, K. C., Linden, J., and Wells, J. N. (1996) *Mol. Pharmacol. 50*, 789−798.
8. Dohlman, H. G., Caron, M. G., Strader, C. D., Amlaiky, N., and Lefkowitz, R. J. (1988) *Biochemistry 27*, 1813−1817.
9. Rong, Y., Arbabian, M., Thiriot, D. S., Seibold, A., Clark, R. B., and Ruoho, A. E. (1999) *Biochemistry 38*, 11278−11286.
10. Servant G., Laporte, S. A., Leduc, R., Escher, E., and Guillemette, G. (1997) *J. Biol. Chem. 272*, 8653−8659.
11. Laporte, S. A., Boucard, A. A., Servant, G., Guillemette, G., Leduc, R., and Escher, E. (1999) *Mol. Endocrinol. 13*, 578−586.
12. Ji, Z., Hadac, E. M., Henne, R. M., Patel, S. A., Lybrand, T. P., and Miller, L. J. (1997) *J. Biol. Chem. 272*, 24393−24401.
13. Hadac, E. M., Pinon, D. I., Ji, Z., Holicky, E. L., Henne, R. M., Lybrand, T. P., and Miller, L. J. (1998) *J. Biol. Chem. 273*, 12988−12993.
14. Janovick, J. A., Haviv, F., Fitzpatrick, T. D., and Conn, P. M. (1993) *Endocrinology 133*, 942−945.
15. Zhou, A. T., Bessalle, R., Bisello, A., Nakamoto, C., Rosenblatt, M., Suva, L. J., and Chorev, M. (1997) *Proc. Natl. Acad. Sci. U.S.A. 94*, 3644−3649.
16. Behar, V., Bisello, A., Bitan, G., Rosenblatt, M., and Chorev, M. (2000*) J. Biol. Chem. 275*, 9−17.
17. Dong, M., Wang, Y., Hadac, E. M., Pinon, D. I., Holicky, E., and Miller, L. J. (1999) *J. Biol. Chem.* 274, 19161−19167.
18. Dong, M., Wang, Y., Pinon, D. I., Hadac, E. M., and Miller, L. J. (1999) *J. Biol. Chem. 274*, 903−909.
19. Li, Y. M., Marnerakis, M., Stimson, E. R., and Maggio, J. E. (1995) *J. Biol. Chem. 270*, 1213−1220.
20. Phalipou, S., Cotte, N., Carnazzi, E., Seyer, R., Mahe, E., Jard, S., Barberis, C., and Mouillac, B. (1997) *J. Biol. Chem. 272*, 26536−26544.
21. Schwartz, T. W. (1994) *Curr. Opin. Biotechnol. 5*, 434−444.
22. Cascieri, M. A., Fong, T. M., and Strader, C. D. (1995) *J. Pharmacol. Toxicol. Methods 33*, 179−185.
23. Strader, C. D., Fong, T. M., Tota, M. R., Underwood, D., and Dixon, R. A. (1994) *Annu. Rev. Biochem. 63*, 101−132.
24. Baldwin, J. M. (1994) *Curr. Opin. Cell Biol. 6*, 180−190.
25. Schwartz, T. W., and Rosenkilde, M. M. (1996) *Trends Pharmacol. Sci. 17*, 213−216.
26. Bossé, R., Servant, G., Zhou, L.-M., Guillemette, G., and Escher, E. (1993) *Regul. Pept. 44*, 215−223.
27. Fraker, P. J., and Speck, J. C. (1978) *Biochem. Biophys. Res. Commun. 80*, 849−857.
28. Laporte, S. A., Servant, G., Richard, D. E., Escher, E., Guillemette, G., and Leduc, R. (1996) *Mol. Pharmacol. 49*, 89−95.
29. Servant, G., Dudley, D. T., Escher, E., and Guillemette, G. (1996) *Biochem. J. 313*, 297−304.
30. Servant, G., Boulay, G., Bosse, R., Escher, E., and Guillemette, G. (1993) *Mol. Pharmacol. 43*, 677−683.
31. Blanton, M. P., and Cohen, J. B. (1994) *Biochemistry 33*, 2859−2872.
32. Clark, M., Cramer, R. D., III, and Opdenbosh, N. V. (1989) *J. Comput. Chem. 10*, 982−1012.
33. Gasteiger, J., and Marcil, M. (1981) *Org. Magn. Reson. 15*, 353−360.
34. Yamano, Y., Ohyama, K., Kikyo, M., Sano, T., Nakagomi, Y., Inoue, Y., Nakamura, N., Morishima, I., Guo, K.-F., Hamakubo, T., and Inagami, T. (1995) *J. Biol. Chem. 270*, 14024−14030.
35. Schwartz, T. W., Gether, U., Schambye, H. T., and Hjorht, S. A. (1995) *Curr. Pharm. Des. 1*, 325−342.
36. Lanctot, P. M., Leclerc, P. C., Escher, E., Leduc, R., and Guillemette, G. (1999) *Biochemistry 38*, 8621−8627.
37. Regoli, D., Park, W. K., and Rioux, F. (1974) *Pharmacol. Rev. 26*, 69−123.
38. Hjorth, S. A., Schambye, H. T., Greenlee, W. J., and Schwartz, T. W. (1994) *J. Biol. Chem. 269*, 30953−30959.
39. Yamano, Y., Ohyama, K., Kikyo, M., Sano, T., Nakagomi, Y., Inoue, Y., Nakamura, N., Morishima, I., Guo, D. F., Hamakubo, T., and Inagami, T. (1995) *J. Biol. Chem. 270*, 14024−14030.
40. Feng, Y. H., Noda, K., Saad, Y., Liu, X. P., Husain, A., and Karnik, S. S. (1995*) J. Biol. Chem. 270*, 12846−12850.
41. Kage, R., Leeman, S. E., Krause, J. E., Costello, C. E., and Boyd, N. D. (1996) *J. Biol. Chem. 271*, 25797−25800.
42. Behar, V., Bisello, A., Bitan, G., Rosenblatt, M., and Chorev, M. (2000) *J. Biol. Chem. 275*, 9−17.
43. Behar, V., Bisello, A., Rosenblatt, M., and Chorev, M. (1999) *Endocrinology 140*, 4251−4261.
44. Hunyady, L., Ji, H., Jagadeesh, G., Zhang, M., Gaborik, Z., Mihalik, B., and Catt, K. J. (1998) *Mol. Pharmacol. 54*, 427−434.
45. Li, Y. M., Marnerakis, M., Stimson, E. R., and Maggio, J. E. (1995) *J. Biol. Chem. 270*, 1213−1220.
46. Laemmli, U. K. (1970) *Nature 227*, 680−685.

BI000597V